JOURNAL OF GEOPHYSICAL RESEARCH, VOL. , NO. , PAGES 1?? ,

Identification of Interplanetary Coronal Mass Ejections at 1 AU Using Multiple Solar Wind Plasma Composition Anomalies

I. G. Richardson[1] and H. V. Cane[2]

NASA Goddard Space Flight Center, Greenbelt, Maryland

Abstract.

We investigate the use of multiple simultaneous solar wind plasma compositional anomalies, relative to the composition of the ambient solar wind, for identifying interplanetary coronal mass ejection (ICME) plasma. We first summarize the characteristics of several solar wind plasma composition signatures (O^{+7}/O^{+6}, Mg/O, Ne/O, Fe charge states, He/p) observed by the ACE and WIND spacecraft within the ICMEs during 1996 – 2002 identified by *Cane and Richardson* [2003], hereafter CR03. We then develop a set of simple criteria that may be used to identify such compositional anomalies, and hence potential ICMEs. To distinguish these anomalies from the normal variations seen in ambient solar wind composition, which depend on the wind speed, we compare observed compositional signatures with those "expected" in ambient solar wind with the same solar wind speed. This method identifies anomalies more effectively than the use of fixed thresholds. The occurrence rates of individual composition anomalies within ICMEs range from $\sim 70\%$ for enhanced iron and oxygen charge states to $\sim 30\%$ for enhanced He/p (> 0.06) and Ne/O, and are generally higher in magnetic clouds than other ICMEs. Intervals of multiple anomalies are usually associated with ICMEs, and provide a basis for the identification of the majority of ICMEs. We estimate that CR03, who did not refer to composition data, probably identified $\sim 90\%$ of the ICMEs present. However, around 10% of their ICMEs have weak compositional anomalies, suggesting that the presence of such signatures does not provide a necessary requirement for an ICME. We note a remarkably similar correlation between the Mg/O and O^7/O^6 ratios in hourly-averaged data both within ICMEs and the ambient solar wind. This "universal" relationship suggests that a similar process (such as minor ion heating by waves inside coronal magnetic field loops) produces the first-ionization potential bias and ion freezing-in temperatures in the source regions of both ICMEs and the ambient solar wind.

1. Introduction

Interplanetary coronal mass ejections (ICMEs), the interplanetary counterparts of coronal mass ejections (CMEs) at the Sun, are characterized by several signatures, as reviewed for example by *Gosling* [1990], *Neugebauer and Goldstein* [1997], and *Zurbuchen and Richardson* [2004]. Solar wind plasma signatures of ICMEs include abnormally low proton temperatures [*Gosling et al.*, 1973; *Richardson and Cane*, 1995], low electron temperatures [*Montgomery et al.*, 1974], and bidirectional suprathermal electron strahls (BDEs) [e.g., *Zwickl et al.*, 1983; *Gosling et al.*, 1987].

Plasma compositional anomalies have also been identified in ICMEs [*Bame*, 1983; *Galvin*, 1997; *Zurbuchen et al.*, 2003]. These include enhanced helium abundances relative to protons [*Hirshberg et al.*, 1972; *Borrini et al.*, 1982] and occasional enhancements in minor ions, in particular iron [*Bame et al.*, 1979; *Mitchell et al.*, 1983; *Ipavich et al.*, 1986; *Neukomm*, 1998; *Wurz et al.*, 2001]. Enhanced Fe charge states have also been reported [*Bame et al.*, 1979; *Fenimore*, 1980; *Ipavich et al.* 1986; *Lepri et al.*, 2001; *Reinard et al.*, 2001; *Lepri and Zurbuchen*, 2004]. On the other hand, a small subset of ICMEs include intervals of unusually ion low charge states, such as He^+ [*Zwickl et al.*, 1982; *Cane et al.*, 1986; *Burlaga et al.*, 1998; *Gloeckler et al.*, 1999; *Ho et al.*, 2000].

Solar wind compositional measurements are of interest because, as reviewed by *Bochsler* [2000], they reflect conditions prevailing near the Sun during the acceleration of the solar wind and the formation of ICMEs. In particular, ion charge states tend to "freeze-in" near the Sun since ionization and recombination time-scales become larger than the solar wind ion expansion time as the coronal electron density decreases with increasing distance from the Sun. The ratio of different ionization states then provides information on the coronal electron temperature at the freezing-in altitude [e.g., *Hundhausen et al.*, 1968; *Owocki et al.*, 1983]. Solar wind ion compositions generally follow photospheric abundances but show a factor of ~ 2 to ~ 4 enrichment (for

[1]Also at Department of Astronomy, University of Maryland, College Park.

[2]Also at School of Mathematics and Physics, University of Tasmania, Hobart, Australia.

Paper number .
0148-0227/04/$9.00

fast or slow solar wind, respectively) relative to photospheric abundances in elements with first ionization potential (FIP) below the Lyman-α limit (10.2 eV). This "FIP-effect" suggests that ions and atoms in chromospheric material are separated before this material is accelerated in the corona, though the details of this process are still under investigation [*von Steiger*, 1998; *Bochsler*, 2000, and references therein]. The FIP effect has also been observed within ICMEs [*Galvin*, 1997; *Neukomm*, 1998].

Recently, *Cane and Richardson* [2003], hereafter CR03, made a comprehensive survey of ICMEs in the near-Earth solar wind during 1996 – 2002, encompassing the increasing and maximum phases of solar cycle 23. Some 214 ICMEs were identified, principally on the basis of solar wind plasma proton signatures (e.g., presence of abnormally low proton temperatures, association with interplanetary shocks) and magnetic field observations. See CR03 for further discussion of the identification of these events. Solar wind composition data, however, were not referred to.

In this paper, we first summarize composition measurements made within the CR03 ICMEs, focusing on ~hourly-averaged data from instruments on the Advanced Compositional Explorer (ACE) and WIND spacecraft. In particular, we compare plasma compositions, and their variability, in the subsets of the CR03 ICMEs with or without "magnetic cloud" signatures. Magnetic clouds have simple flux-rope like magnetic fields characterized by enhanced magnetic fields that rotate slowly through a large angle. Such events [*Burlaga et al.*, 1981; *Klein and Burlaga*, 1982] have been identified for example by the WIND magnetometer team (see http://lepmfi.gsfc.nasa.gov/mfi/mag_cloud_pub1.html).

We then compare the ICME compositions with those in the "ambient" solar wind outside ICMEs. Ambient solar wind compositional signatures are generally ordered by the solar wind speed (for example, O^7/O^6 and Mg/O are anti-correlated with V_{sw} [e.g., *Geiss et al.*, 1995]). We find that these dependences are essentially independent of the phase of the solar cycle, at least during the period considered in this paper (the He/p ratio is a notable exception). This enables us to summarize ambient solar wind compositions in terms of "expected" or average values which are ~ time-independent functions of the solar wind speed. ICMEs typically have plasma compositional signatures that exceed expected values in ambient solar wind with the same solar wind speed.

We then assess whether departures of ~hourly-averaged plasma composition measurements relative to such expected values provide a practical means of routinely identifying ICMEs. Recently, *Lepri et al.*, [2001] and *Lepri and Zurbuchen* [2004] have demonstrated that intervals of enhanced iron charge states are closely associated with ICMEs. However, here we consider additional, multiple compositional signatures in concert. We also examine whether compositional signatures indicate the presence of additional ICMEs that were not identified by CR03 or, conversely, whether there are CR03 events with unusually weak compositional signatures.

In the next section we describe the observations used in this investigation. In Section 3, variations in the compositional signatures in magnetic clouds, non-cloud ICMEs, and the ambient solar wind as a function of solar wind speed are summarized, while Section 4 discusses the use of compositional anomalies in ICME identification. Section 5 examines the average spatial relationship between compositional anomalies and the CR03 ICMEs. Section 6 notes the similar relationship between variations in the O^7/O^6 and Mg/O ratios in the ambient solar wind and within ICMEs which may have important implications for understanding the origin of the compositional signatures of ICMEs. The results are summarized in Section 7.

2. Instrumentation

The plasma composition observations used in this paper are principally from the Solar Wind Ion Composition Spectrometer (SWICS) [*Gloeckler et al.*, 1998] on the ACE spacecraft, launched in August 1997. "Level 2" SWICS data, obtained from the ACE Science Center (http://www.srl.caltech.edu/ACE/ASC/), include 1-hour averages of the O^{+7}/O^{+6}, $^{24}Mg^{+10}/O^{+6}$, C^{+5}/C^{+6} and $^{20}Ne^{+8}/O^{+6}$ ratios at the time of writing. These data are examined up to December 2002, the end of the period discussed by CR03.

We also use a summary of iron charge states measured by SWICS and averaged over two-hour intervals, an update of the data set used by *Lepri et al.* [2001]. The parameters provided are the mean Fe charge state $< Q_{Fe} >$ and the fraction of Fe ions that have charge states ≥ 16. The data considered here extend to the end of 2001.

Richardson et al. [2003a] reported that on occasion, enhanced values of the SWICS Level 2 C^5/C^6 ratio (implying low carbon freezing-in temperatures) are found inside ICMEs even though other elements such as oxygen and iron simultaneously exhibit enhanced freezing-in temperatures. This apparently anomalous behavior of the carbon charge states now appears to be an instrumental effect requiring further investigation (T. Zurbuchen, private communication, 2004). Thus, we will not discuss the C^5/C^6 ratio further in this paper.

To help place the composition observations in context, we use observations from the ACE magnetometer and Solar Wind Electron, Proton, and Alpha Monitor (SWEPAM), as well as from the National Space Science Data Center (NSSDC) "OMNI2" solar wind data-base (http://nssdc.gsfc.nasa.gov/omniweb/). This incorporates inter-calibrated plasma and magnetic field data from ACE and other near-Earth spacecraft with a time resolution of 1 hour. The time offset between the ACE and OMNI2 data, corresponding to the solar wind travel time from ACE to the Earth, is typically less than the 1-hour resolution of both the observations considered here and the ICME times given by CR03, and can be neglected for the purposes of this study.

We also use data from the MIT WIND instrument (courtesy of J. Richardson) to provide information on the He/proton ratio prior to the start of ACE observations.

Note that in the results presented in this paper, we have made several minor updates to the CR03 list. First, two additional ICMEs in late 2002 (December 17, 1800 – December 19, 1200, and December 21, 0300 – December 22, 1900) have been added, while a questionable event on November 10 – 11, 2000 has been removed after review of additional solar wind data. A few minor corrections have also been made to the parameters in the published CR03 list.

3. Abundance variations with solar wind speed

As has been demonstrated previously, compositional variations in the ambient solar wind are generally ordered by

solar wind speed [e.g., *Geiss et al.*, 1995]. Thus it is interesting to compare solar wind abundance variations both in the ambient solar wind and ICMEs as a function of the concurrent solar wind speed. For example, Figure 1 shows hourly-averaged values of the SWICS O^7/O^6 ratio during 1998 – 2002 plotted vs. solar wind speed in "ambient" solar wind (Figure 1(a)), the CR03 non-magnetic cloud ICMEs (Figure 1(b)), and magnetic clouds (Figure 1(c)) (cf. the similar results of *Reisenfeld et al.* [2003] for ICME and ambient solar wind regions identified by the Genesis spacecraft on-board solar wind regime algorithm).

The ambient solar wind (81% of the SWICs data points) shows the well-known anti-correlation between the O^7/O^6 ratio and solar wind speed, corresponding to lower freezing-in temperatures in faster solar wind [e.g., *Geiss et al.*, 1995; *Gloeckler et al.*, 2003]. (The "quantization" at low O^7/O^6 ratios results from the two decimal place accuracy of the Level 2 data.) Since ICME boundaries are sometimes difficult to locate exactly, the "ambient" solar wind considered here excludes intervals $\leq$ 8 hours before and after the CR03 ICMEs. The average dependence of the O^7/O^6 ratio vs. solar wind speed may be summarized by the log-linear fit to the O^7/O^6 vs. V_{sw} distribution, with O^7/O^6 chosen as the dependent variable, shown in Figure 1(a) and repeated for reference in Figures 1(b-c).

The distribution for magnetic clouds (Figure 1(c); 3.3% of the SWICS data points) is distinctly different, showing a weak positive correlation in O^7/O^6 with solar wind speed. For a given solar wind speed, O^7/O^6 is generally higher than average values in the ambient solar wind (as indicated by the fit to the distribution in Figure 1(a)). Even at lower speeds ($<\sim$ 400 km/s), although the magnetic cloud distribution overlies that for the ambient solar wind, values of O^7/O^6 are still generally above average ambient solar wind values. Typical O^7/O^6 ratios are $\sim$ 1 in magnetic clouds, with the majority lying in a range from $\sim$ 0.2 to $\sim$ 8.

Non-cloud ICMEs (Figure 1(b); 9.7% of the SWICS data points) show an intermediate behavior. Values of O^7/O^6 in non-cloud ICMEs are generally above average values in the ambient solar wind, which in turn approximately define the lower limits of O^7/O^6 for a given solar wind speed both in these ICMEs and magnetic clouds. However, values of O^7/O^6 are more variable than in magnetic clouds and show little correlation with solar wind speed, the best fit suggesting if anything a very weak decrease in O^7/O^6 with increasing solar wind speed.

Enhancements in O^7/O^6 have previously been reported by *Henke et al.* [1998, 2001] in magnetic clouds observed by the Ulysses spacecraft. As they also note, relative to values in the ambient solar wind with the same speed, the O^7/O^6 ratio is more strongly enhanced in faster magnetic clouds. However, we find enhanced values of O^7/O^6 (relative to those in the ambient solar wind) within both magnetic clouds and other ICMEs, contrary to their conclusion that magnetic clouds, but not other ICMEs, are characterized by enhanced O^7/O^6.

We have also summarized other compositional signatures in the same way. Figure 2 shows distributions of $^{24}Mg^{+10}/O^{6+}$ vs. solar wind speed. The well known anticorrelation between the Mg/O ratio and solar wind speed [e.g., *Geiss et al.*, 1995] is evident in the ambient solar wind (Figure 2(a)), reflecting the reduced enhancement of low FIP elements, such as magnesium, in faster solar wind. The distributions for magnetic clouds and other ICMEs follow remarkably similar patterns to the equivalent distributions for O^7/O^6 even though one parameter reflects freezing-in temperatures, the other the FIP effect (we will return to this point in Section 6). Magnetic clouds (Figure 2(c)) show variable values of Mg/O that are predominantly above average solar wind values and have a weak correlation with solar wind speed suggesting an overall increase in the FIP effect in faster magnetic clouds. Non-cloud ICMEs (Figure 2(b)) show even more variation in Mg/O, with values that generally lie above average values in the ambient solar wind, but have little trend with solar wind speed (see also the similar results of *Reisenfeld et al* [2003] for Genesis ICMEs).

Ne/O (Figure 3) shows evidence of a weak anti-correlation with solar wind speed in ambient solar wind. Similar to O^7/O^6 and Mg/O, values of Ne/O in ICMEs are variable but tend to lie above average ambient solar wind values, with a weak positive correlation and less variability evident in magnetic clouds.

We show in Figure 4 2-hourly averages of the fraction of iron ions with charge states $\geq$ 16 (Figure 4(a)) and the mean iron charge state (Figure 4(b)), both plotted versus solar wind speed, in ambient solar wind, non-cloud ICMEs, and magnetic clouds during 1998 – 2001. The ambient solar wind distributions for both parameters are consistent with a trend towards lower Fe charge states (suggesting lower freezing-in temperatures) in faster solar wind. In contrast, magnetic clouds show a clear trend towards higher values of these parameters (indicating higher Fe freezing-in temperatures) in faster events, well above average values in the ambient solar wind. Non-cloud ICMEs show more variability, though values again lie predominantly above average values in the ambient solar wind. There is even a hint of a bimodal behavior in that, while the majority of points lie above the distribution in the ambient solar wind, a minority appear to be more consistent with the corresponding ambient solar wind values.

Lepri et al. [2001] chose a criterion of $(Fe \geq 16)/Fe_{tot} \geq 0.1$ to define intervals of enhanced Fe charge state, and noted that such intervals were usually associated with ICMEs included in a preliminary version of the CR03 list. Although this criterion rejects ambient solar wind data points fairly well (only $\sim$ 16% of ambient solar wind data meet this criterion), Figure 4(a) indicates that a substantial fraction ($\sim$ 36%) of non-cloud ICME points will also be rejected. *Lepri et al.* [2001] also used a minimum interval duration of 20 hours, and noted that although $\sim$ 90% of the intervals defined by their criteria were associated with ICMEs, only $\sim$ 50% of the ICMEs in their list were associated with such features. However, we note that other ICMEs do typically have shorter periods of enhanced Fe charge states, and that 113/156 (72%) of the CR03 ICMEs for which we have Fe charge state data have event-average values of $(Fe \geq 16)/Fe_{tot} \geq 0.1$. Thus the association rate of CR03 ICMEs with enhanced Fe charge states is higher than is suggested by *Lepri et al.* [2001]. See also *Lepri and Zurbuchen* [2004], who report that, of a subset of 57 of the CR03 ICMEs, 75% were associated with enhanced Fe charge states as defined by an interval of $< Q_{Fe} > > 12$ for at least 6 consecutive hours, as well as the results to be presented below.

Event averages of the parameters in Figures 1 – 4 also show trends similar to those evident in the higher time resolution data. Thus, the corresponding plots are not reproduced here. In particular, magnetic clouds show relatively

well ordered, increasing trends in O^7/O^6, Mg/O, Ne/O and the iron charge states with increasing average ICME speed, while non-cloud ICMEs show more variation and weaker trends with increasing solar wind speed (declining for O^7/O^6, Mg/O and Ne/O, and increasing for Fe charge states).

Another interesting feature of the parameters in Figures 1 – 4 is that the solar wind speed dependences in the ambient solar wind are essentially time-independent. We have examined the fits to O^7/O^6, Mg/O, Ne/O, $Fe \geq 16/Fe_{tot}$, and $< Q_{Fe} >$ versus V_{sw} in ambient solar wind for each year when data are available, as well as for some shorter periods and for the complete period of interest, and find that the fit parameters are essentially independent of the period chosen. This means that a single signature vs. V_{sw} dependence can be assumed for a given compositional signature in the ambient solar wind throughout the study period. To characterize this dependence for each signature, we choose the fit for the year or longer period that gives the highest correlation with the solar wind speed. The fit parameters adopted, and period over which they are obtained, are summarized in Table 1.

The final compositional signature that we will consider is the He/proton ratio. Studies over many years have noted that enhanced values of the He/p ratio (e.g., above 8%) are associated with structures that we now identify with ICMEs [e.g., *Hirshberg et al.*, 1972; *Borrini et al.*, 1982]. An interesting feature of the He/p ratio in the ambient solar wind is that, in contrast to the other compositional signatures discussed above, the solar wind speed variation has a clear solar cycle dependence. Figure 5(a) shows the evolution of the He/proton vs. V_{sw} distribution in the ambient solar wind during one-year intervals between 1996 (solar minimum) and 2000 (solar maximum). The observations are from the MIT instrument on the WIND spacecraft. The distribution changes from one in which He/p increases with solar wind speed at solar minimum to one where the ratio is more enhanced and essentially independent of solar wind speed near solar maximum. This evolution of the He/p ratio both as a function of solar cycle and solar wind speed is also illustrated in different formats by *Aellig et al.* [2001] and *Richardson et al.* [2003b]. A solar cycle variation in He/p has also been noted previously by, for example, *Feldman et al.* [1978].

Figure 5(b) shows the evolution of the WIND He/p ratio in ICMEs (both cloud and non-cloud) during the same period. This ratio is highly variable but the distributions of He/p basically overlap those in the ambient solar wind, and evolve in a similar way, also tending towards larger He/p and less variation with solar wind speed at higher solar activity levels (as also noted by *Richardson et al.* [2003b]). The data support the conclusions of previous studies that higher values of He/p tend to be associated with ICMEs rather than the ambient solar wind. A threshold of $He/p = 0.06$, for example, indicated by the horizontal lines in Figure 5, excludes the majority of ambient solar wind data. On the other hand, it is clear that only a subset of ICME data points meet this criterion, while the majority of points overlie the ambient solar wind distribution. This implies that the He/p ratio alone is not a particularly useful means of reliably distinguishing ICME material from ambient solar wind. The solar cycle variation in the He/p ratio and considerable overlap between ICME and ambient solar wind values is in marked contrast to the behavior of the other compositional signatures and suggests that the helium abundance in the ambient solar wind and ICMEs is determined by processes that are essentially unrelated to freezing in temperatures or the FIP effect. One possibility is the degree of gravitational settling of helium, which is less strongly coupled to the outward solar wind flow than other ions [e.g., *Neugebauer and Goldstein*, 1997].

4. Compositional anomalies and ICME identification

Having compared and contrasted several compositional signatures of ambient solar wind and ICMEs, we now consider how such signatures can be used to identify ICMEs.

One method might be to define an arbitrary threshold value, for example O^7/O^6=0.8, which excludes the vast majority of the ambient solar wind data points (Figure 1a). However, this criterion will also exclude some ICME points that fall below this threshold but still have elevated values of O^7/O^6 relative to the ambient solar wind with the same speed.

Another method that has been used in some previous studies [e.g., *Henke et al.*, 1998, 2001] is to compare the ICME composition with that of the ambient solar wind upstream and downstream of the ICME. However, this comparison seems somewhat arbitrary since there is likely to be a greater contrast between the ICME and upstream solar wind compositions if the surrounding solar wind has a high, rather than a low, speed (cf., Figure 1).

The method we will examine here is to compare the relative value of a compositional signature measured at a given time in solar wind of a particular speed with the "expected" value for ambient solar wind with the same speed. To determine the expected values, we use the fits to the signature - V_{sw} distributions given in Table 1. To illustrate the method, Figure 6 shows solar wind data for a representative period in May – June, 2000. Standard solar wind magnetic field and plasma parameters are shown at the top of the figure. The beginning of this period was dominated by slow solar wind then by a corotating high-speed stream commencing late on May 29. Subsequently, four ICMEs were identified by CR03 during June 5 – 14 at the times indicated by gray shading.

Figures 6(h-k) show the O^7/O^6, Mg/O, Ne/O, and $Fe \geq 16/Fe_{tot}$ ratios measured by ACE/SWICS. Superimposed on the observed values are the expected values inferred from the fit parameters in Table 1 and the simultaneously observed solar wind speed. Note that the expected values tend to track compositional variations fairly well in the ambient (non-ICME) solar wind which, in particular, is prominent early in Figure 6. Deviations from normal solar wind composition can also be readily identified in this presentation, in particular periods with signatures that are significantly enhanced above expected values. These in turn are generally closely associated with CR03 ICMEs, as would be expected from the distributions presented in Figures 1 – 4.

Determining when the difference between the observed and expected values of a signature is sufficient to be judged as "anomalous" is somewhat arbitrary. For the purposes of this paper, we will assume that a criterion of $\geq$ twice the expected value identifies anomalous values of O^7/O^6, Mg/O, Ne/O, and $Fe \geq 16/Fe_{tot}$. For $< Q_{Fe} >$, we use $< Q_{Fe} > \geq < Q_{Fe} >_{exp} +1$. Inspection of Figures 1 – 4 suggests that these criteria are likely to separate ICME and

ambient solar wind data fairly well. However, we recognize that there will still be ICME intervals with near-solar wind compositions that will not be identified in this way.

We note that an essentially similar method of ICME identification was recently suggested by *Gloeckler et al.* [2003]. They demonstrated that the speed of the ambient solar wind and the electron temperature in the solar wind source region, inferred from the Ulysses SWICS O^7/O^6 ratio using a model calculation, are related by $V_{sw}^2 \sim 1/T$. Such a relationship is also predicted by the solar wind model of *Fisk* [2003]. *Gloeckler et al.* [2003] noted in passing that ICME intervals during their study period deviated from this relationship between V_{sw} and T, specifically having higher freezing-in temperatures than expected from the solar wind speed, and made the suggestion that comparison of V_{sw} and T could provide a basis for the routine identification of ICMEs. The essential difference in our approach is that the O^7/O^6 ratio is used directly, rather than first converted to a model-dependent freezing-in temperature. We also consider additional compositional signatures.

Since the $He/p - V_{sw}$ relationship is not time-independent, we cannot use a similar method to identify anomalous He/p intervals. Instead, here we simply use a criterion of $He/p \geq 0.06$, based on the results in Figure 5, to identify strongly enhanced helium abundances that are typically associated with ICMEs. However, as discussed above, only a subset of observations within ICMEs have such abundances. Values of He/p are shown in Figure 6(g) (the horizontal dashed line indicates He/p=0.06). Most of the CR03 ICMEs in Figure 6 have $He/p > 0.06$.

Note that this method of identifying compositional anomalies relative to "expected" values typical of the ambient solar wind is analogous to the technique we have used in many studies to identify periods of anomalously low plasma proton temperature in the solar wind, which are also frequently associated with ICMEs/MCs [e.g., *Richardson and Cane,* 1995]. This technique compares the observed plasma proton temperature with the expected value (T_{exp}) in normally expanding solar wind with the same solar wind speed. Figure 6(d) shows the proton temperature with T_{exp}, based on the *Lopez* [1987] analysis of the $V_{sw} - T_p$ correlation in the OMNI data, superposed. Black shading denotes abnormally cool regions ($T_p/T_{ex} \leq 0.5$). These typically correspond to CR03 ICMEs since the presence of abnormally cool plasma is an important ICME signature considered by CR03.

In addition to considering each compositional signature separately, it is also interesting to sum up the total number of abnormal composition signatures (maximum = 6) that are observed during each 1-hour interval, based on the criteria discussed above. (Since the Fe charge-state data are 2-hour averages, the same values are assumed to hold for each 1-hour sub-interval.) The total number of signatures is shown in Figure 6(l). It is evident that intervals with several coincident signatures are generally closely associated with CR03 ICMEs, as would be expected from the analysis discussed above.

Figure 7 summarizes the compositional signatures that are judged to be anomalous, based on the above criteria, in hourly-averaged data during a longer period, July-December, 2000. At the top of the figure, the times of ICMEs suggested by CR03 are indicated. Again, we emphasize that these times were inferred principally from examination of solar wind plasma and magnetic field observations, without reference to the compositional data. Below are shown the total number of anomalous compositional signatures, and the times when individual signatures (He/p, enhanced Fe and O charge states, Mg/O, and Ne/O) are judged to be anomalous. Again, the various anomalies tend to occur together, and intervals of multiple solar wind compositional anomalies typically agree reasonably well with the identified ICMEs. This result can be regarded in two ways: if anomalous compositions are indeed general signatures of ICME plasma, then the results such as in Figures 6 and 7 suggest that the ICME identifications of CR03 were reasonably reliable. Alternatively, if the CR03 ICME identifications are assumed to be reliable, then the results indicate that ICME plasma is typically associated with plasma anomalies, essentially the starting point for this paper. Note also there is no single signature that is obviously consistently superior in selecting ICMEs, and might be examined to the exclusion of other signatures. In fact, at least during the interval in Figure 7, the "classic" signature of enhanced He/p appears to be as successful at identifying putative ICMEs as the compositional anomalies inferred from SWICS data. Hence, we suggest that such a method of comparing anomalies in several compositional signatures (as available) relative to expected ambient solar wind values provides a useful tool for inferring the presence of ICMEs in the solar wind.

Nevertheless, there are occaisional intervals of compositional anomalies that are not associated with CR03 ICMEs. In some cases, these "anomalies" arise from data that, on further examination, are clearly unreliable (for example, have erratic point-to-point variations). Prominent examples occur at times of unusually low plasma densities when SWICS is unable to make reliable measurements. Unfortunately, the current SWICS Level 2 data do not include estimates of the accuracy of individual measurements which might allow unreliable data to be identified during the analysis. More interestingly, some other anomalies may be indicative of ICMEs that were not identified by CR03, and these merit further attention. For example, between February, 1998, the start of the SWICS Level 2 data, and the end of 2002, we identify 17 intervals, defined by the criterion that $\geq$ 60% of the signatures for which data are available (i.e., making allowance for data gaps in certain signatures) are anomalous for at least 12 hours, with any break in continuity lasting less than 3 hours, that were not associated with CR03 ICMEs. These events are listed in Table 2.

Several of the events during 1998 – 2000 in Table 2 are associated with enhanced Fe charge state intervals identified by *Lepri et al.* [2001] that were not coincident with CR03 ICMEs but were suggested to be ICMEs based on the presence of BDEs. This close comparison between the events not associated with CR03 ICMEs inferred in these separate studies is not too surprising given that iron charge state data are common to both, and that the various compositional signatures tend to occur together.

The event on January 23 – 24, 2000, closely follows a CR03 ICME, so it is arguable whether it is really unrelated to the previously identified ICME. Interestingly, *Richardson et al.* [2003a] pointed out that this feature forms part of a "recurrent" sequence of similar compositional anomalies in the slow solar wind ahead of a corotating high-speed stream, previous events (also noted by *Lepri et al.* [2001]) being evident on November 30 – December 2 and December 26 to 28, 1999. Although BDEs were present during these recurrent events, suggesting an association with ICMEs, it is unclear how to reconcile the recurrent nature of these events with

an ICME origin, though further consideration of this topic is beyond the scope of this paper. In any case, making the assumption that all the events in Table 2 are ICMEs that were not identified by CR03, they amount to $\sim$ 10% of the number of events (183) identified by CR03 during the same period. This at least suggests that a significant number of ICMEs (as revealed by compositional anomalies following criteria such as those above, and excluding "anomalies" due to unreliable data) were not overlooked by CR03.

There are also occasional CR03 ICMEs with relatively weak compositional signatures. For example, if we require a period of at least 3 hours duration with at least > 20% of signatures anomalous, then only 17 ($\sim$ 9%) of the 179 CR03 ICMEs during February 1998 – 2002 (with data available) do not meet this criterion. These ICMEs with exceptionally weak compositional signatures are listed in Table 3 (with parameters extracted from Table 1 of CR03). A re-examination of the magnetic field and plasma data for these events shows that several are among the weaker (i.e., less distinct, more questionable) of the CR03 events. Nevertheless, the lack of compositional anomalies should not inevitably lead to the conclusion that these events are not ICMEs. For example, the ICME on April 21 – 23, 2001 is a cataloged WIND magnetic cloud. Interestingly, this occurred during an active period when many of the ICMEs passing ACE did have strong compositional signatures ($\sim$ 100% of available signatures), while others did not. Likewise, the October 1 – 2, 2001 ICME is one of a sequence of three ICME intervals during September 30 – October 3 (CR03), but shows weaker compositional anomalies than the adjacent ICMEs. Several of the events in Table 3 are also associated with LASCO halo CMEs and moderate geomagnetic storms.

The January 22 and March 10, 2000 ICMEs are immediately followed by periods of anomalous compositions (cf. Table 2). These ICMEs were principally identified by their low T_p signature, but this may indicate only part of a larger ICME suggested by the compositional signatures. (*Richardson et al.* [2003a] show additional examples of ICMEs where the region of abnormally low T_p is only a substructure of the complete ICME.)

Around 76% of the ICMEs in Table 3 have speeds $\leq$ 400 km/s, compared with $\sim$ 30% of all the CR03 ICMEs in the analysis interval, and only one has a speed above 500 km/s. Thus, these events tend to be slower than typical ICMEs. The lack of compositional anomalies in these events does not arise simply because the compositions of ICMEs and slow solar wind tend to overlap (cf. Figures 1 – 4). Rather, the compositional signatures are intrinsically weak. Many of the event durations are also relatively short – $\sim$ 40% have durations $\leq$ 12 hours, and only three (18%) have durations more than 1 day.

In summary, we suggest that the identification of solar wind compositional anomalies by a method such as that described above, comparing observed compositions with reference to those in ambient solar wind with the same speed, is a valuable method of routinely identifying potential ICME-related material, although a small minority ($\sim$ 10%) of ICMEs may only include weak compositional signatures. The analysis also suggests that the CR03 ICME list most likely includes a majority of events, and that most of the identifications are most likely reliable, although determination of the ICME boundaries may benefit from perusal of the composition data, as noted in the next Section. After excluding intervals of apparently poor quality data, we estimate that CR03 may have missed around 10% of ICMEs based on the occurrence of intervals of compositional anomalies unrelated to the identified ICMEs.

5. Spatial Relationship of Intervals of Anomalous Composition and CR03 ICMEs

Figure 8 summarizes the percentage of data points (summed over all CR03 ICMEs for which the relevant data are available) for which various compositional signatures are judged to be anomalous as a function of the location relative to the CR03 ICME boundaries, expressed as a percentage of the duration of the ICME (i.e., 0%= ICME leading edge; 100%=ICME trailing edge).

Overall, the ICME boundaries suggested by CR03 tend to order the boundaries of the regions of anomalous composition. In addition, the anomaly occurrence rates within ICMEs vary with the signature considered, with Ne/O and He/p showing the lowest rates ($\sim$ 30%) and enhanced iron charge states and O^7/O^6 the highest rates ($\sim$ 70%). Figure 8 also suggests that, on average, the occurrence of anomalous O^7/O^6, Mg/O and Ne/O decreases from the leading to the trailing edge of ICMEs. Although this may indicate a general spatial trend in composition within ICMEs, we also note that the tendency for the solar wind speed to decline during the passage of an ICME (due to ICME expansion) will cause the "expected" values of the compositional signatures to increase with time. This in turn raises the threshold required for the composition to be judged as anomalous, which might be expected to cause, on average, a decrease in the anomaly occurrence rate with time during ICME passage.

The relatively low occurrence rate of $He/p \geq 0.06$ inside ICMEs might be anticipated from Figure 5. Interestingly, the average occurrence rate tends to increase towards the ICME trailing edge. Furthermore, enhanced helium abundances are rarely detected ahead of the ICME, while there is evidence of a region trailing the ICME, extending to $\sim$ 50% of the ICME duration, in which the probability of observing enhanced He/p is higher than in the ambient solar wind. This analysis suggests that strongly enhanced helium abundances are more likely to occur towards the trailing edge of, and possibly trailing, ICMEs (a pattern that appears to be evident during the first two CR03 ICMEs in Figure 6). This spatial distribution may be consistent with the hypothesis that enhanced He/p is the result of gravitational settling of helium. Other compositional signatures may show a tendency towards extending into the region behind the ICME trailing edge (*Richardson et al.* [2003a] noted that enhanced Fe charge states tend to extend beyond the trailing edges of some CR03 ICMEs), but the predominant (average) pattern is for the major decrease in the occurrence rate of compositional anomalies to take place in the vicinity of the suggested ICME trailing edge.

Where compositional anomalies are identified in the region immediately outside of the CR03 ICMEs, several effects may contribute: First, the ICME boundaries may be in error; reassessment of these boundaries taking the compositional signatures into consideration may improve their accuracy. Alternatively, compositional signatures may in fact extend beyond the ICME boundaries that are most clearly defined by plasma/field features. A further factor may be important in the post-shock sheath immediately ahead of

an ICME: The "expected" values of most of the composition parameters discussed above will *decrease* at the abrupt speed increase associated with the shock/disturbance. In some cases, this decrease may be sufficient for the anomaly criterion (e.g., twice the expected value) to be met, even when there is no actual change in the plasma composition. An example is seen around midday on June 8, 2000 in Figure 6 – the major compositional signature (apparently a substructure of the CR03 ICME) starts around a day later. This effect contributes to the number of apparently anomalous data points ahead of some ICMEs, and is responsible for the increases in occurence rates, most prominent in O^7/O^6 and $Fe \geq 16/Fe_{tot}$, at $\sim -100\%$ with respect to the ICME location in Figure 8. We suggest that a more sophisticated algorithm to flag the leading edge of a compositional anomaly should also require a change in the value of the composition parameter.

An important point to infer from Figure 8 is that a shock/disturbance standing off upstream of an ICME is usually propagating through solar wind that does not have an anomalous (i.e., ICME-like) composition. This appears to be inconsistent with the proposal of *Boberg et al.* [1996] that high iron charge states in solar particle events are accelerated by ICME-driven shocks out of a source population of ICME-like material that somehow leaks upstream from the ICME, notwithstanding, of course, that occasionally, a shock will happen to propagate through plasma associated with an unrelated preceding ICME.

6. A "Universal" Relationship Between O^7/O^6 and Mg/O in Ambient Solar Wind and ICMEs

In Section 3, we noted the similar characteristics of the distributions for O^7/O^6 and Mg/O versus solar wind speed in Figures 1 and 2 in both the ambient solar wind and ICMEs. This is despite the fact that these ratios characterize freezing-in temperatures or FIP-biases, respectively, that arise from different physical processes. Pursuing this further, in Figure 9 we show hourly averages of Mg/O plotted versus O^7/O^6 in the ambient solar wind, non-cloud ICMEs, and magnetic clouds. The plots show a high degree of correlation, even in the hourly-averaged data, between Mg/O and O^7/O^6 in all these regions. In particular, note that the considerable scatter in the data points for non-cloud ICMEs in Figures 1 and 2 is largely removed, suggesting that this scatter is largely due to correlated variations in Mg/O and O^7/O^6 within ICMEs that are not in turn well-ordered by the solar wind speed.

A particularly interesting feature of Figure 9 is that the relationship between Mg/O and O^7/O^6, indicated for example by the best fits through the data, is essentially identical both in the ambient solar wind and within non-cloud ICMEs and magnctic clouds. The main difference is a deficiency of smaller values of Mg/O and O^7/O^6 in ICMEs. This apparently "universal" relationship is remarkable because (1) the FIP effect and oxygen charge states are determined by conditions in different regions of the solar atmosphere, and (2) if ICMEs are formed of closed magnetic structures which do not encounter conditions (e.g., electron temperatures) in the ambient corona, the ion charge state distributions might be expected to develop in a different manner from those in the ambient solar wind [*Neukomm and Bochsler*, 1996]. Thus, it is not immediately obvious that FIP and ion charge states will be similarly related both inside ICMEs and in the ambient solar wind.

Somewhat surprisingly, the results in Figure 9 seem inconsistent with the conclusion of *Reinard et al.* [2001] that there is no correlation between the event-averaged SWICS Fe/O ratio, another measure of the size of the FIP effect (not available in the current Level 2 data), and the O^7/O^6 ratio in the ICMEs they studied in 1998 – 1999. They suggested that the presence of a correlation between the size of the FIP effect and oxygen freezing-in temperature may be dependent on the stage of the solar cycle. However, we find that O^7/O^6 and Mg/O are correlated throughout the period we have examined (1998 – 2002), providing no evidence of such a cycle dependence. A possibility that might explain the different results is that the *Reinard et al.* [2001] ICME identifications were based on BDEs observed by ACE. Although we do not know the exact periods they examined, we note that events on the publically available ACE BDE list (http://www.bartol.udel.edu/~chuck/ace/ACElists/obs_list.html) may differ considerably from the periods identified by CR03, possibly because of complications in interpreting counterstreaming electron observations [*Gosling et al.*, 2001], and include what we would classify as non-ICME flows.

A recent theoretical model [*Schwadron et al.*, 1999] suggests a possible explanation for the correlation between FIP bias and ion freezing-in temperatures in the ambient solar wind. This involves wave heating of minor ions inside coronal magnetic field loops to a degree that is correlated with the loop size. The material within these loops is then released by reconnection with open field lines as required by the heliospheric magnetic field model of *Fisk*, [1996]. Such loops are observed to be larger in the source regions of the slow solar wind than in the regions (coronal holes) that give rise to fast solar wind, where field lines are predominantly open. Thus, slow solar wind plasma is characterized by higher freezing-in temperatures and a larger FIP bias than fast solar wind (cf. Figures 1(a) and 2(a)). The model of *Fisk* [2003] incorporates these conjectures and predicts that $V_{sw}^2 \sim 1/T$, as found observationally by *Gloeckler et al.* [2003] using T derived from oxygen charge states.

The apparently "universal" relationship between Mg/O and O^7/O^6 suggests that such a process may also operate on the plasma within ICMEs. This plasma may be contained on magnetic field loops that are themselves ejected into the solar wind as a CME, as distinct from the draining of plasma along newly opened field lines in the source of the slow solar wind. Possibly, some CMEs/ICMEs may result from exceptionally large coronal loops that have more pronounced compositional signatures than the ambient solar wind [e.g., *Gloeckler et al.*, 2003]. However, the tight relationship between the compositional signatures and solar wind speed evident in the ambient solar wind (and predicted by the *Fisk* [2003] model) clearly breaks down in ICMEs. This is perhaps not too suprising. First, in the Fisk model, the energy to accelerate the ambient solar wind speed comes from the reconnection of open field lines with closed loops. Hence, the final solar wind speed is intimately related to the properties of these loops. On the other hand, if the loops themselves are ejected during the formation of coronal mass ejections, there may be little or no relationship between the speed of the CME and the properties of the constituent loops. Second, ICMEs undergo acceleration near the Sun then tend towards ambient solar wind speeds as they move out through the heliosphere. Hence, ICME speeds observed

in-situ may not reflect conditions during CME formation and release, whereas compositional signatures will do so.

The more ordered, less variable, compositional variations for magnetic clouds compared to non-cloud ICMEs in Figures 1 – 4 might also be consistent with such a scenario: Magnetic clouds have simple magnetic structures. If this in turn reflects a simplicity in the field loop configuration in the related CME at the Sun, then the resulting plasma compositions and charge states arising from heating in these loops are likely to be relatively similar (well-ordered) from event to event, and possibly correlated with the gross properties of the resulting ICME, such as its speed. Non-cloud ICMEs however, often have more complicated structures. One possibility is that non-cloud ICMEs are composed of a complex of separate loops near the Sun that is expelled to form a single CME. Each loop may be heated to a different degree, resulting in variable, though correlated, FIP bias and ion freezing-ion temperatures within the CME which however bare little relationship to the gross properties of the ICME. Some non-cloud ICMEs might also consist of a conglomeration of initially separate "interacting" CMEs with different compositions.

There is also a degree of correlation between the He/p and O^7/O^6 ratios. Figure 10 shows distributions of both hourly-averaged and event-averaged values of these parameters for the CR03 ICMEs. Though there is certainly a great deal of scatter, there is a tendency for higher helium enhancements to be associated with higher values of O^7/O^6, in particular in the event averages (*Reinard et al.* [2001] report a similar result). Thus, the conditions that lead to strongly enhanced oxygen freezing-in states during the formation of ICMEs also appear to be conducive to the release of plasma with high helium abundances. We also note that *Lepri and Zurbuchen* [2004] have recently suggested that flare heating may play a role in generating enhanced ion charge states, in particular for iron, within ICMEs. However, it is unclear whether the universal relationship between the FIP effect and ion charge states (as indicated by Mg/O and O^7/O^6) is consistent with different processes heating plasma within ICMEs and the source regions of the ambient solar wind.

7. Summary

We have examined the relationship between the ICMEs/magnetic clouds identified by CR03 and solar wind plasma compositional anomalies including He/p, O^7/O^6, Mg/O, Ne/O and iron charge states. These anomalies (with the exception of He/p) are inferred by comparing the observed compositional paramters with "expected" values based on the normal variation in composition with solar wind speed in the ambient solar wind, which we conclude is essentially independent of the phase of the solar cycle, at least in 1998 – 2002. We find that:

- Plasma within both magnetic clouds and non-cloud ICMEs tends to be characterized by higher freezing-in temperatures and FIP biases than in ambient solar wind with the same speed. Magnetic clouds as a group show a more consistent behavior (for example with respect to ICME speed), and less event-to-event or hour-to-hour variation, than other ICMEs. Our results contrast with the conclusion of *Henke et al.* [1998, 2001] based on Ulysses observations, that magnetic clouds, but not other ICMEs, show enhancements in ion charge states compared to the ambient solar wind.

- The He/p distribution for ICMEs shows a considerable overlap with that of the ambient solar wind, and both distributions tend to evolve to higher values of He/p as solar activity levels increase. Values of $He/p \geq 0.06$ are predominantly restricted to ICMEs and are relatively rare in the ambient solar wind. However, only $\sim$ 30% of plasma within ICMEs meets this criterion.

- Comparing observed hour-to-hour variations in composition parameters such as O^7/O^6, Mg/O, Ne/O and Fe charge states relative to expected values in the ambient solar wind provides a useful method of distinguishing intervals of anomalous composition from those variations inherent in the ambient solar wind (cf. the technique suggested by *Gloecker et al.* [2003] based on comparing oxygen freezing-in temperatures and the solar wind speed).

- Intervals of multiple compositional anomalies tend to be associated with the ICMEs identified by CR03, though additional events are also present (perhaps $\sim$ 10% of the number of ICMEs identified by CR03). This result may be interpreted as indicating that CR03 identified the majority of ICMEs present, and that, more importantly, the identification of compositional anomalies provides a promising tool for indicating the presence of ICME material in the solar wind that may be more objective than some methods currently in use, which render ICME-identification as "something of an art" [*Gosling,* 1997]. However, compositional anomalies are very weak/not present in a small subset (perhaps $\sim$ 10%) of ICMEs, suggesting that the presence of such anomalies does not provide a necessary criterion for an ICME.

- The compositional signatures most frequently found in ICMEs are enhanced iron and oxygen charge states ($\sim$ 70% of data points). However, there is no single compositional signature among those considered that is outstandingly successful at identifying anomalies associated with ICMEs and might be used alone as a tracer of ICMEs in the solar wind. Thus, consideration of multiple signatures is a reasonable approach.

- On average, the boundaries of the CR03 ICMEs organize the intervals of compositional anomalies, although compositional anomalies may extend beyond these boundaries in individual events.

- Generally, the He/p ratio is more likely to be enhanced above 0.06 towards, and in a region beyond, the ICME trailing edge.

- Shocks/disturbances upstream of ICMEs usually lie in solar wind that has an ambient solar wind-like, rather than ICME-like, composition. The composition of the sheath between the shock and ICME leading edge is also that of the ambient solar wind. Hence, energetic particles accelerated out of the solar wind by an ICME-driven shock should reflect an ambient solar wind, not an ICME, source population (an obvious exception is the case when the shock happens to be propagating through an unrelated ICME).

- There appears to be a "universal" relationship between O^7/O^6 (i.e., ion freezing-in temperature) and Mg/O (i.e., FIP bias) both within ambient solar wind and ICMEs, suggesting that a similar process (such as that proposed by *Schwadron et al.* [1999]) heats minor ions in both ICMEs and the ambient solar wind. However, the close relationship between composition and speed variations found in the ambient solar wind (and predicted by the model of *Fisk* [2003]) does not hold in ICMEs. The greater variation in composition within non-cloud ICMEs compared to magnetic clouds may reflect more complicated magnetic loop structures (e.g., multiple loops of various heights) within the associated CMEs at the Sun.

In conclusion, solar wind plasma observations clearly hold promise as a tool for routine identification of ICMEs in the solar wind. The event-to-event variations in composition, and the close correlations between different signatures are likely to provide important information on conditions during the formation of CMEs that will no doubt be the focus of future studies.

Acknowledgments.
H.V.C. was supported at GSFC by a contract with USRA, and I.G.R. was supported by NASA grant NCC 5-180. A NASA Sun-Earth Connections Guest Investigator Award is also acknowledged. We thank Thomas Zurbuchen and Sue Lepri for useful discussions.

References

Aellig, M. R., A. J. Lazarus, and J. T. Steinberg, The solar wind helium abundance: variation with wind speed and the solar cycle, *Geophys. Res. Lett., 28*, 2767, 2001.

Bame, S. J., Solar wind minor ions – recent observations, in *Solar Wind 5 Proceedings*, ed. M. Neugebauer, NASA Conf. Proc. 2280, p. 573, 1983.

Bame, S. J., J. R. Asbridge, W. C. Feldman, E. E. Fenimore, and J. T. Gosling, Solar wind heavy ions from flareheated coronal plasma, *Sol. Phys., 62*, 179, 1979.

Boberg, P. R., A. J. Tylka, and J. H. Adams, Jr., Solar energetic Fe charge state measurements: Implications for acceleration by coronal mass ejection-driven shocks, *Astrophys. J. Lett., 471*, L65, 1996.

Bochsler, P., Abundances and charge states of particles in the solar wind, *Rev. Geophys., 38*, 247, 2000.

Borrini, G., J. T. Gosling, S. J. Bame, and W. C. Feldman, Helium abundance enhancements in the solar wind, *J. Geophys. Res., 87*, 7370, 1982.

Burlaga, L. F., E. Sittler, F. Mariani, and R. Schwenn, Magnetic loop behind an interplanetary shock: Voyager, Helios and Imp 8 observations, *J. Geophys. Res., 86*, 6673, 1981.

Burlaga, L. F., et al, A magnetic cloud containing prominence material: January 1997, *J. Geophys. Res., 103*, 227, 1998.

Cane, H. V., and I. G. Richardson, Interplanetary coronal mass ejections in the near-earth solar wind during 1996-2002, *J. Geophys. Res., 108(4),*, 10.1029/2002JA009817, 2003.

Cane, H. V., S. W. Kahler, and N. R. Sheeley, Jr., Interplanetary shocks preceded by solar filament eruptions, *J. Geophys. Res., 91*, 13,3231, 1986.

Cane, H. V., I. G. Richardson, and O. C. St. Cyr, Coronal mass ejections, interplanetary ejecta, and geomagnetic storms, *Geophys. Res. Lett., 27*, 3591, 2000.

Feldman, W. C., J. R. Asbridge, S. J. Bame, and J. T. Gosling, Long-term variations of selected solar wind properties: Imp 6, 7 and 8 results, *J. Geophys. Res., 83*, 2177, 1978.

Fenimore, E. E., Solar wind flows associated with hot heavy ions, *Astrophys. J., 235*, 245, 1980.

Fisk L. A., Acceleration of the solar wind as a result of the reconnection of open magnetic flux with coronal loops, *J. Geophys. Res., 108 (A4)*, 1157, doi:10.1029/2002JA009284, 2003.

Galvin, A. B., Minor ion composition in CME-related solar wind, in *Coronal Mass Ejections*, eds. N. Crooker, J. A. Joselyn, and J. Feynman, AGU., Washington DC, p. 253, 1997.

Geiss, J., G. Gloeckler, and R. von Steiger, Origin of the solar wind from composition data, *Space Sci. Rev., 72*, 49, 1995.

Gloeckler, G., et al., Investigation of the composition of solar and interstellar matter using solar wind and pickup ion measurements with SWICS and SWIMS on the ACE spacecraft, *Space Sci. Rev., 86*, 495, 1998.

Gloeckler, G., et al., Unusual composition of the solar wind in the 2 - 3 May 1998 CME observed with SWICS on ACE, *Geophys. Res. Lett. 26*, 157, 1999.

Gloeckler, G., T. H. Zurbuchen, and J. Geiss, Implications of the observed anticorrelation between solar wind speed and coronal electron temperature, *J. Geophys. Res., 108(A4)*, 1158, doi:10.1029/2002JA009286, 2003.

Gosling, J. T., Coronal mass ejections and magnetic flux ropes in interplanetary space, in *Physics of Magnetic Flux Ropes*, Geophys. Monogr. Ser., vol. 58, edited by C. T. Russell, E. R. Priest, and L. C. Lee, p. 343, AGU, Washington, D. C., 1990.

Gosling, J. T., Coronal mass ejections: An overview, in *Coronal Mass Ejections*, Geophys. Monogr. Ser., vol. 99, edited by N. Crooker, J. A. Joselyn, and J. Feynman, p. 9, AGU, Washington D. C., 1997.

Gosling, J. T., V. Pizzo, and S. J. Bame, Anomalously low proton temperatures in the solar wind following interplanetary shock waves Evidence for magnetic bottles?, *J. Geophys. Res., 78*, 2001, 1973.

Gosling, J. T., R. M. Skoug, and W. C. Feldman, Solar wind electron halo depletions at 90° pitch angle, *Geophys. Res. Lett., 28*, 4155, 2001.

Henke, T., J. Woch, U. Mall, S. Livi, B. Wilken, R. Schwenn, G. Gloeckler, R. von Steiger, R. J. Forsyth, and A. Balogh, Differences in the O^{+7}/O^{+6} ratio of magnetic cloud and noncloud coronal mass ejections, *Geophys. Res. Lett., 25*, 3465, 1998.

Henke, T., J. Woch, R. Schwenn, U. Mall, G. Gloeckler, R. von Steiger, R. J. Forsyth, and A. Balogh, Ionization state and magnetic topology of coronal mass ejections, *J. Geophys. Res., 106*, 10,597, 2001.

Hirshberg, J., S. J. Bame, and D. E. Robbins, Solar flares and solar helium enrichments: July 1965 - July 1967, *Sol. Phys., 23*, 467, 1972.

Ho, G. C., D. C. Hamilton, G. Gloeckler, and P. Bochsler, Enhanced solar wind $^3He^{2+}$ associated with coronal mass ejections, *Geophys. Res. Lett., 27*, 309, 2000.

Hundhausen, A. J., H. E. Gilbert, and S. J. Bame, Ionization state of the interplanetary plasma, *J. Geophys. Res., 73*, 5485, 1968.

Ipavich, F. M., A. B. Galvin, G. Gloeckler, D. Hovestadt, S. J. Bame, B. Klecker, M. Scholer, L. A. Fisk, and C. Y. Fan, Solar wind Fe and CNO measurements in high-speed flows, *J. Geophys. Res., 91*, 4133, 1986.

Klein, L. W., and L. F. Burlaga, Interplanetary magnetic clouds at 1 AU, *J. Geophys. Res., 87*, 613, 1982.

Lepping, R. P., J. A. Jones, and L. F. Burlaga, Magnetic field structure of interplanetary magnetic clouds at 1 AU, *J. Geophys. Res., 95*, 11,957, 1990.

Lepri, S. T., and T. H. Zurbuchen, Iron charge state distributions as an indicator of hot ICMEs: Possible sources and temporal and spatial variations during solar maximum, *J. Geophys. Res., 109*, No. A1, A01112, 10.1029/2003JA009954, 2004.

Lepri, S. T., T. H. Zurbuchen, L. A. Fisk, I. G. Richardson, H. V. Cane, and G. Gloeckler, Iron charge distribution as an identifier of interplanetary coronal mass ejections, *J. Geophys. Res., 106*, 29,231, 2001.

Lopez, R. E., Solar cycle invariance in solar wind proton temperature relationships, *J. Geophys. Res., 92*, 11,189, 1987.

Mitchell, D. G., E. C. Roelof, and S. J. Bame, Solar wind iron abundance variations at speeds > 600 km sec^{-1}, 1972 – 1976, *J. Geophys. Res., 88*, 9059, 1983.

Neugebauer, M., and R. Goldstein, Particle and field signatures of coronal mass ejections in the solar wind, in *Coronal Mass Ejections*, eds. N. Crooker, J. A. Joselyn, and J. Feynman, AGU., Washington DC, 245, 1997.

Neukomm, R. O., Composition of coronal mass ejections derived with SWICS/Ulysses, Ph.D. Thesis, University of Bern, 1998.

Neukomm, R. O., and P. Bochsler, Diagnostics of closed magnetic structures in the solar corona using charge states of helium and minor ions, *Astrophys. J., 465*, 462, 1996.

Owocki, S. P., T. E. Holzer, and A. J. Hundhausen, The solar wind ionization state as a coronal temperature diagnostic, *Astrophys. J., 275*, 354, 1983.

Reinard, A. A., T. H. Zurbuchen, L. A. Fisk, S. T. Lepri, R. M. Skoug, and G. Gloeckler, Comparison between average charge states and abundances of ions in CMEs and the slow solar wind, in *Solar and Galactic Composition*, ed. R. F. Wimmer-Schweingruber, American Inst. Phys. Proc. Vol. 598, AIP, Melville, NY, p. 139, 2001.

Reisenfeld, D. B., J. T. Steinberg, B. L. Barraclough, E. E. Dors, R. C. Wiens, M. Neugebauer, A. Reinard, and T. Zurbuchen, Comparison of the Genesis solar wind regime algorithm results with solar wind composition observed by ACE, in *Solar Wind Ten*, eds. M. Velli, R. Bruno, and F. Malara, American Inst. Phys. Proc. Vol. 679, AIP, Melville, NY, p. 632, 2003.

Richardson, I. G., and H. V. Cane, Regions of abnormally low proton temperature in the solar wind (1965-1991) and their association with ejecta, *J. Geophys. Res., 100,* 23,397, 1995.

Richardson, I. G., H. V. Cane, S. T. Lepri, T. H. Zurbuchen, and J. T. Gosling, Spatial relationship of signatures of interplanetary coronal mass ejections, in *Solar Wind Ten,* eds. M. Velli, R. Bruno, and F. Malara, American Inst. Phys. Proc. Vol. 679, AIP, Melville, NY, p. 681, 2003a.

Richardson, J. D., I. G. Richardson, J. C. Kasper, H. V. Cane, N. U. Crooker, and A. J. Lazarus, Helium variation in the solar wind. Solar Variability as an Input to the Earth's Environment, *Proc. Sci. Comm. on Solar-Terrestrial Phys., International Solar Cycle Studies Symposium 2003,* European Space Agency *ESA SP-535,* 521, 2003b.

Schwadron, N. A., L. A. Fisk, and T. H. Zurbuchen, Elemental fractionation in the slow solar wind, *Astrophys. J., 521,* 859, 1999.

von Steiger, R., Composition aspects of the upper solar atmosphere: Rapporteur paper III, *Space Sci. Rev., 85,* 407, 1998.

von Steiger, R., R. F. Wimmer-Schweingruber, J. Geiss, and G. Gloeckler, Abundance variations in the solar wind, *Adv. Space Res., 15(7),* 3, 1995.

Wurz, P., R. F. Wimmer-Schweingruber, K. Issautier, P. Bochsler, A. B. Galvin, J. A. Paquette, and F. M. Ipavich, Composition of magnetic cloud plasmas during 1997 and 1998, in *Solar and Galactic Composition,* ed. R. F. Wimmer-Schweingruber, American Inst. Phys. Proc. Vol. 598, AIP, Melville, NY, p. 145, 2001.

Zurbuchen, T. H., and I. G. Richardson, In-situ solar wind and magnetic field signatures of interplanetary coronal mass ejections, *Space Science Rev.,* in press, 2004.

Zurbuchen, T. H., L. A. Fisk, S. T. Lepri, and R. von Steiger, The composition of interplanetary coronal mass ejections, in *Solar Wind Ten,* eds. M. Velli, R. Bruno, and F. Malara, American Inst. Phys. Proc. Vol. 679, AIP, Melville, NY, p. 604, 2003.

Zwickl, R. D., J. R. Asbridge, S. J. Bame, W. C. Feldman, and J. T. Gosling, He^+ and other unusual ions in the solar wind: A systematic search covering 19721980, *J. Geophys. Res.,* 87, 7379, 1982.

Zwickl, R. D., J. R. Asbridge, S. J. Bame, W. C. Feldman, J. T. Gosling, and E. J. Smith, Plasma properties of driver gas following interplanetary shocks observed by ISEE3, in *Solar Wind Five*; NASA Conference Proceedings 2280, edited by M. Neugebauer, p. 711, NASA, Washington, D. C., 1983.

H. V. Cane and I. G. Richardson, Laboratory for High Energy Astrophysics, Code 661, NASA Goddard Space Flight Center, Greenbelt, MD, 20771 (hilary.cane@utas.edu.au; richardson@lheavx.gsfc.nasa.gov)

(Received _____.)

Table 1. Parameters Characterizing "Expected" (Average) Compositional Ratios in Ambient Solar Wind

Signature	V_{sw} Relationship	Fit Interval
O^7/O^6	$\ln(O^7/O^6) = -0.00578V_{sw} + 1.10$	1999
Mg/O	$\ln(Mg/O) = -0.00367V_{sw} - 0.711$	2000
Ne/O	$\ln(Ne/O) = -0.0017V_{sw} - 1.22$	2000
$Fe \geq 16/Fe_{tot}$	$\ln(Fe \geq 16/Fe_{tot}) = -0.00421V_{sw} - 1.23$	1998
$< Q_{Fe} >$	$< Q_{Fe} >= 11.2 - 0.000857V_{sw}$ (i.e., $< Q_{Fe} > \approx 11$)	1998 – 2001

Table 2. $\geq$ 12-Hour Duration Intervals Outside CR03 ICMEs With $\geq$ 60% of Available Signatures Anomalous

Disturbance Time[a] (UT)	Interval Start (UT)	End (UT)	Duration (hours)	*Lepri et al.*?[b]	SW Structure	Notes
1998						
Mar. 30 2200	Mar. 31 0500	Apr. 1 0700	26}	Yes/BDE/ICME	ICME?	T_p depression, $\sim$ radial field
	Apr. 1 1600	Apr. 2 2200	30}	Yes/BDE/ICME	ICME?	ditto
May 17 1800	May 17 1800	May 18 0900	15	No	ICME?	Weak T_p depression
June 8 1300	June 8 1300	June 9 0300	14	No (< 24 hr)	ICME?	BDE[c]
June 8 1300	Sep. 29 0700	Sep. 30 0300	20	No (data gap)	ICME?	Partial data gap; T_p depression
1999						
Jan. 9 0000	Jan. 9 1400	Jan. 11 0300	37	Yes/BDE/ICME	ICME?	Weak plasma/field signatures
Nov. 27. 0400	Nov. 27 0500	Nov. 28 0100	20	Yes/BDE/ICME	ICME?	Weak plasma/field signatures
Nov. 30 0500	Nov. 30 1400	Dec. 1 0800	18	Yes/BDE/ICME	ICME?	Corotating?[d]
2000						
Jan. 22 0023(A)	Jan. 23 1700	Jan. 24 0700	14	Yes/ICME	ICME?	Follows CR03 ICME; Corotating?[d]
Mar. 10 0000	Mar. 11 0500	Mar. 11 1800	13	Yes/ICME?	ICME?	Follows CR03 ICME
Jul 21 0700	Jul 22 0100	Jul 22 1900	18	Yes/ICME	ICME	Weak T_p depression
Aug. 14 2136(A)	Aug 15 1600	Aug 16 0700	15	No	ICME?	Weak plasma/field signatures
Sep 30 0400	Sep 30 0500	Oct 1 0000	19	–	?	Complex plasma/field structure
Dec. 3 0321(A)	Dec. 4 0200	Dec. 4 1600	14	–	ICME?	Weak plasma/field signatures
2001						
Oct. 3 2100	Oct. 4 1400	Oct. 5 2200	32	–	ICME?	T_p depression
Nov. 14 1500	Nov. 14 1500	Nov. 15 1800	27	–	ICME?	Sector boundary
Dec. 6 2200	Dec. 8 1300	Dec. 9 0400	15	–	ICME?	T_p depression; weak signatures
2002						
No Events						

[a] The time of the associated SC when present. Otherwise, 'A' indicates the time of shock passage at ACE. If no shock or SC is reported, the estimated arrival time of the disturbance (which in some cases is also the ICME leading edge) is given to the nearest hour.

[b] *Lepri et al.* [2001] enhanced Fe charge state event (February 1998 – September 2000). BDE – Event not identified in a preliminary version of the CR03 list refered to by *Lepri et al.* [2001], but associated with BDEs, suggesting a possible ICME.

[c] ACE disturbance list, courtesy of C. W. Smith.

[d] *Richardson et al.* [2003a]

Figure 1. Distributions of hourly-averaged values of the O^7/O^6 ratio measured by ACE/SWICS in 1998 – 2002, plotted versus concurrent solar wind speed, for (a) ambient solar wind, (b) ICMEs [*Cane and Richardson*, 2003] that are not magnetic clouds, and (c) ICMEs that are magnetic clouds. The fit to the ambient solar wind distribution is repeated in (b) and (c) and shown together with the fit to the individual distributions.

Figure 2. As Figure 1, but for Mg/O.

Figure 3. As Figure 1, but for Ne/O.

Figure 4. As Figure 1, but for (a) $(Fe \geq 16)/Fe_{tot}$ and (b) $< Q_{Fe} >$ in 1998 – 2001.

Figure 5. Evolution of the WIND $He/p - V_{sw}$ distribution during 1996 – 2000 in (left) the ambient solar wind and (right) all (cloud and non-cloud) CR03 ICMEs.

Figure 6. Solar wind magnetic field, plasma and composition parameters from ACE (1-hour averages) during a representative period in May – June, 2000. Gray shaded intervals denote CR03 ICMEs. "Expected values" of O^7/O^6, Mg/O, Ne/O, $Fe \geq 16/Fe_{tot}$ and $< Q_{Fe} >$ (see text) are overlaid on the observed values. The number of anomalous compositional signatures present is also shown.

Figure 7. Comparison of the intervals during July – December 2000 in which various compositional signatures are judged to be anomalous and the times of CR03 ICMEs. The total number of anomalous signatures is also shown.

Figure 8. Variation of composition anomaly occurrence rates (percentage of data points that are anomalous) for various compositional signatures as a function of time with respect to CR03 ICMEs, with 0% corresponding to ICME leading edge passage and 100% to the ICME trailing edge.

Figure 9. Hourly averages of Mg/O plotted vs. O^7/O^6 for ambient solar wind, non-cloud ICMEs, and magnetic clouds. Note the similar relationship of Mg/O ($\sim$ FIP effect) and O^7/O^6 ($\sim$ oxygen freezing in temperatures) in all these solar wind regions.

Figure 10. Hourly and event-averaged values of He/p plotted vs. O^7/O^6 in ICMEs.

Table 3. CR03 ICMEs in 1998 – 2002 With Weak SWICS Compositional Signatures ($\geq$ 20% of Available Signatures With Duration $\geq$ 3 Hours Not Present).

Disturbance Time (UT)	ICME Start (UT)	ICME End (UT)	Duration (hrs)	V_{ej} (km/s)	B (nT)	MC?	Dst (nT)	V_{tr} (km/s)	LASCO CME[a]
1998									
Feb. 17 0400	Feb. 17 1000	Feb. 17 2100	11	400	12	1	–102	602	Feb. 14 0655
March 06 0300	March 06 1500	March 07 1600	25	330	7	1	–25	...	
Aug. 05 1300	Aug. 05 1300	Aug. 06 1200	23	360	13	1	-166	dg	dg
1999									
June 26 2016	June 27 1400	June 28 1400	24	680	8	0	-43	760	June 24 1331 H
2000									
Jan. 22 0023	Jan. 22 1700	Jan. 23 0200	9	380	16	1	–91	530	Jan. 18 1754 H
March 09 2300	March 10 0100	March 10 0600	5	390	6	1	0	...	
March 18 2200	March 19 0200	March 19 1200	10	380	9	0	-2	...	
June 18 0900	June 18 0900	June 18 1700	8	380	6	1	-9	...	
Oct. 20 1800	Oct. 20 2200	Oct. 21 0800	10	400	4	0	-2	...	
2001									
April 21 1601	April 21 2300	April 23 0800	33	350	11	2	–104	...	
June 07 0852(A)	June 07 1800	June 08 0700	13	390	9	1	–4	...	
July 13 1700	July 13 1700	July 14 0100	8	400	8	1	-8	...	
Aug. 15 0500	Aug. 15 0500	Aug. 16 1400	33	390	5	0	-16	...	
Aug. 27 1952	Aug. 28 2000	Aug. 29 2000	24	470	4	0	-20	810	Aug. 25 1650 H
Sept. 30 1924	Oct. 01 0800	Oct. 02 0000	16	490	9	0	-150	710	Sept. 28 0854 H
Nov. 19 1815	Nov. 19 2200	Nov. 20 1100	13	480	6	1	–32	680	Nov. 17 0530 H
Dec. 29 0538	Dec. 30 0000	Dec. 30 1400	14	400	17	1	-39	570	Dec. 26 0530?
2002									
No events									

[a] 'H' indicates that the CME had a 360° angular extent (i.e. halo CME). '?' indicates that the CME association may be doubtful. Times in brackets indicate associated solar events during an interval with no coronagraph coverage. 'dg' indicates that there was a LASCO data gap around the expected time of the associated CME.

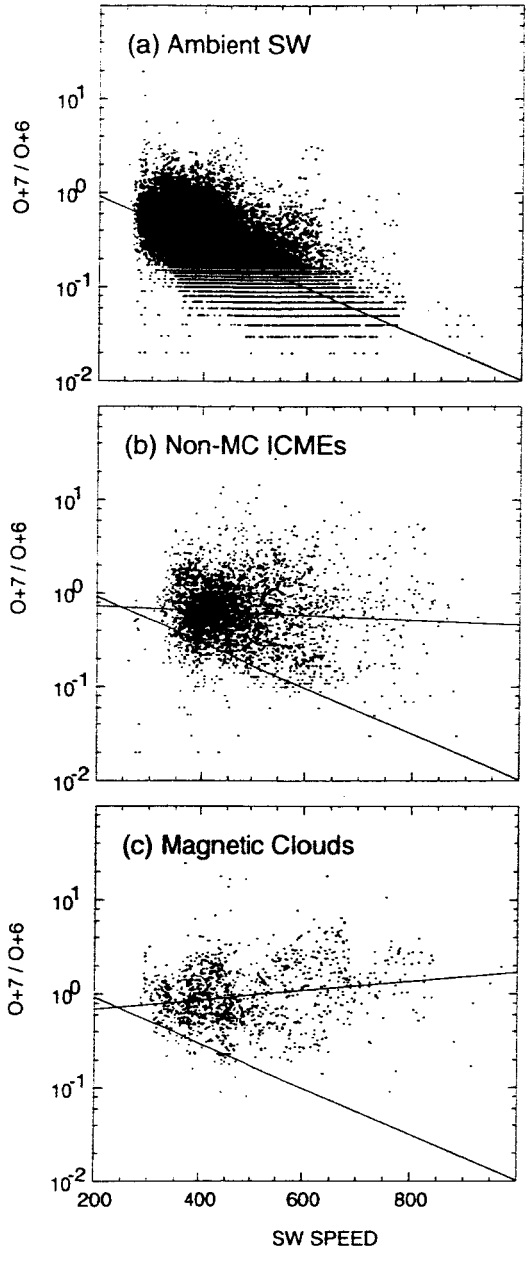
(a) Ambient SW
(b) Non-MC ICMEs
(c) Magnetic Clouds
O+7 / O+6
10^{1}
10^{0}
10^{-1}
10^{-2}
200
400
600
800
SW SPEED

Figure 1

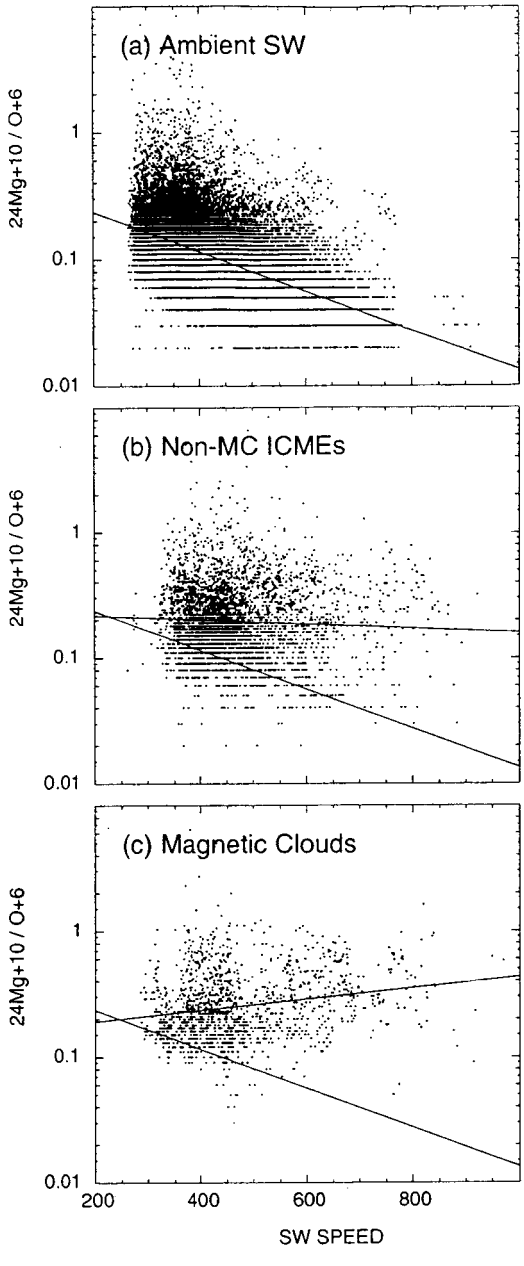
(a) Ambient SW
(b) Non-MC ICMEs
(c) Magnetic Clouds
24Mg+10 / O+6
1
0.1
0.01
200
400
600
800
SW SPEED

Figure 2

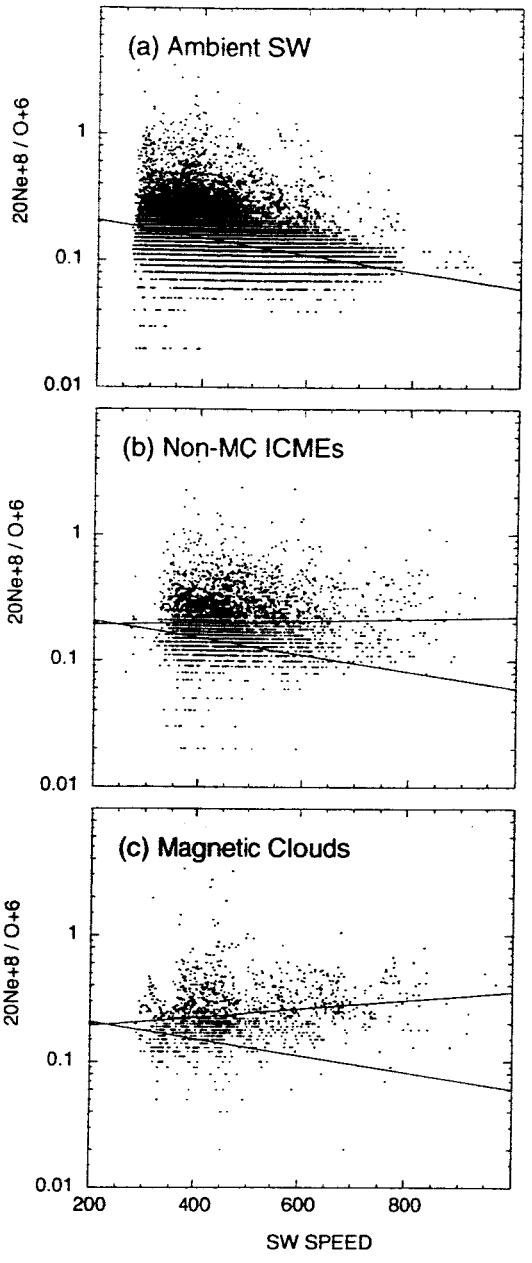
(a) Ambient SW
(b) Non-MC ICMEs
(c) Magnetic Clouds
20Ne+8 / O+6
1
0.1
0.01
200
400
600
800
SW SPEED

Figure 3

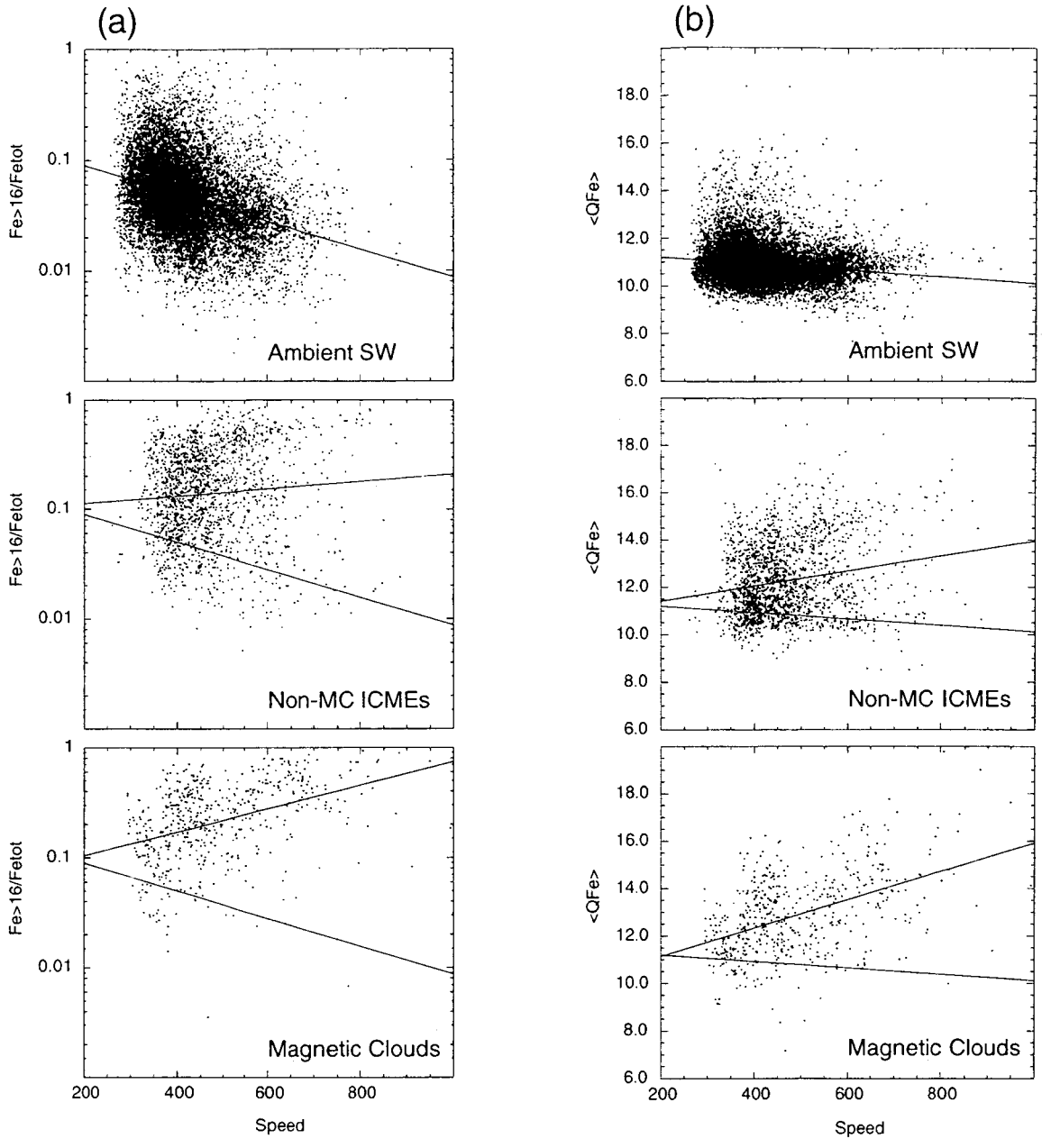
(a)
(b)
Fe>16/Fetot
<QFe>
Ambient SW
Non-MC ICMEs
Magnetic Clouds
Speed
1
0.1
0.01
18.0
16.0
14.0
12.0
10.0
8.0
6.0
200
400
600
800

Figure 4

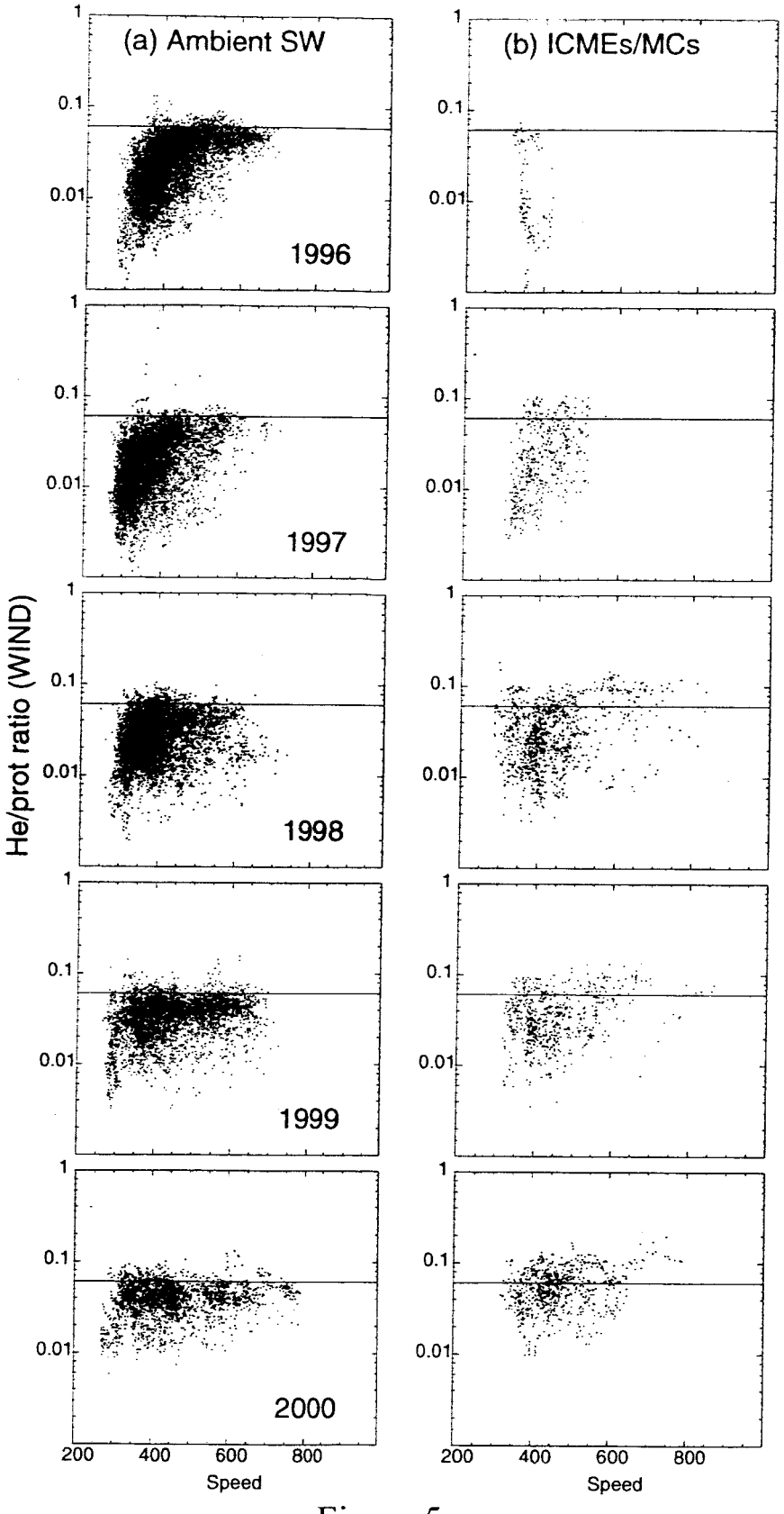
(a) Ambient SW
(b) ICMEs/MCs
1996
1997
1998
1999
2000
He/prot ratio (WIND)
Speed
Speed
1
0.1
0.01
200
400
600
800

Figure 5

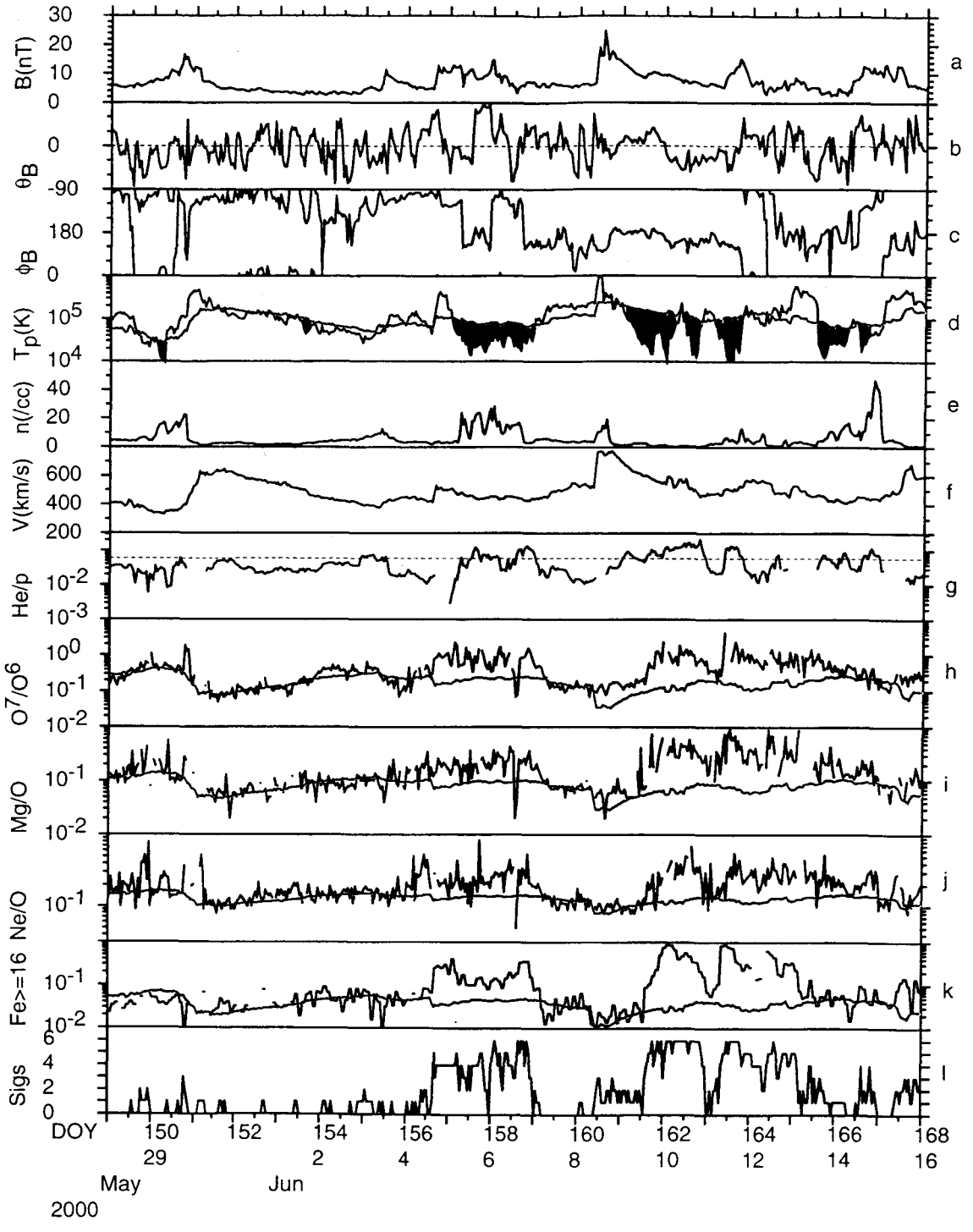
B(nT)
30
20
10
0
a
θB
0
-90
b
φB
180
0
c
Tp(K)
10^5
10^4
d
n(/cc)
40
20
0
e
V(km/s)
600
400
200
f
He/p
10^-2
10^-3
g
O7/O6
10^0
10^-1
10^-2
h
Mg/O
10^-1
10^-2
i
Ne/O
10^-1
j
Fe>=16
10^-1
10^-2
k
Sigs
6
4
2
0
l
DOY
150
152
154
156
158
160
162
164
166
168
29
2
4
6
8
10
12
14
16
May
Jun
2000

Figure 6

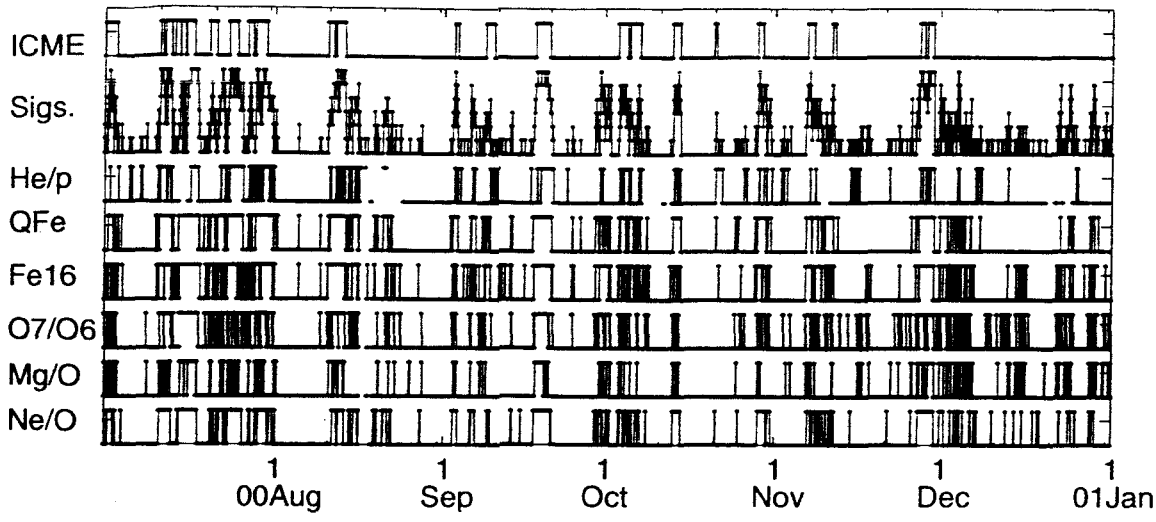
ICME
Sigs.
He/p
QFe
Fe16
O7/O6
Mg/O
Ne/O
1
00Aug
1
Sep
1
Oct
1
Nov
1
Dec
1
01Jan

Figure 7

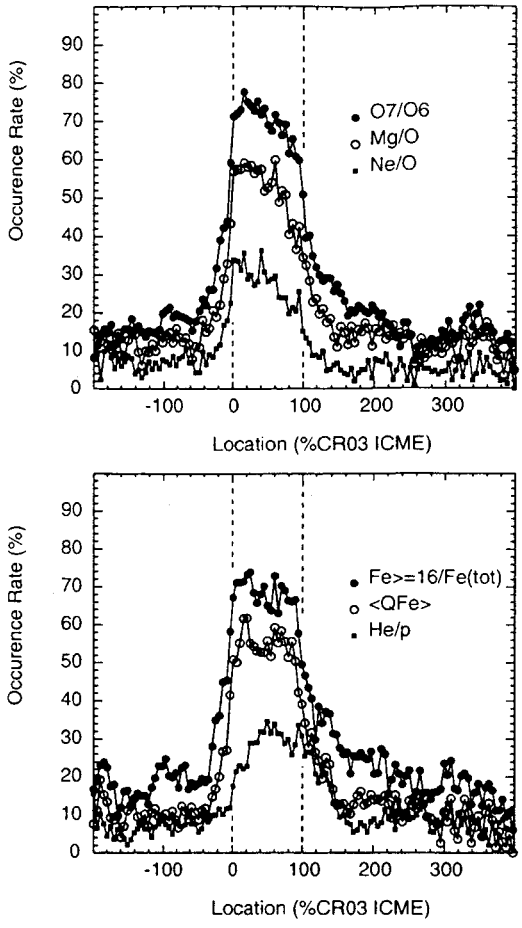
Occurence Rate (%)
90
80
70
60
50
40
30
20
10
0
-100
0
100
200
300
Location (%CR03 ICME)
O7/O6
Mg/O
Ne/O
Occurence Rate (%)
90
80
70
60
50
40
30
20
10
0
-100
0
100
200
300
Location (%CR03 ICME)
Fe>=16/Fe(tot)
<QFe>
He/p

Figure 8

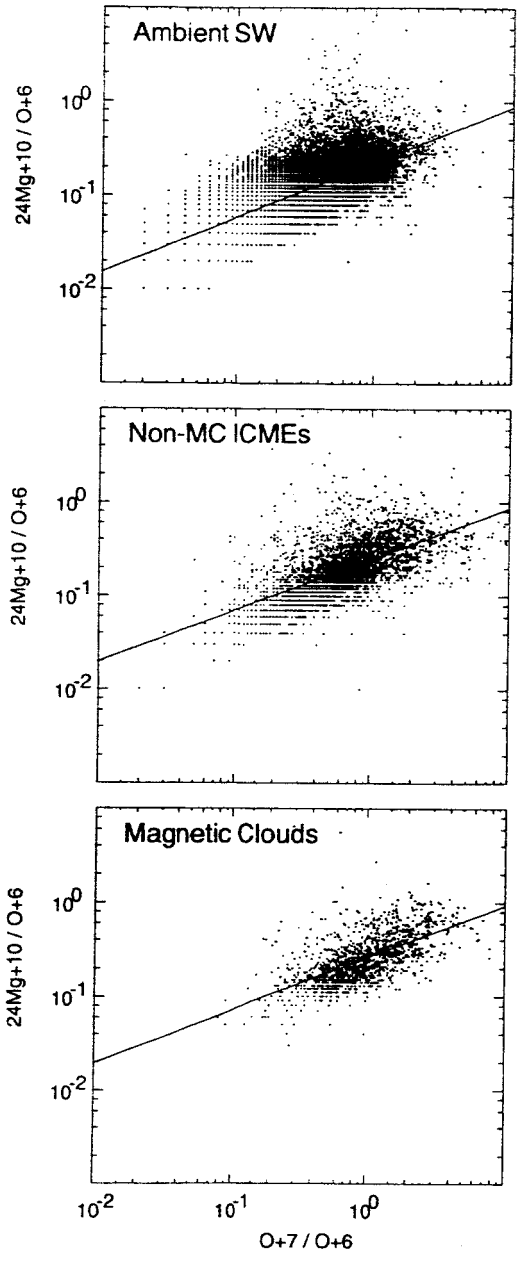
Ambient SW
Non-MC ICMEs
Magnetic Clouds
24Mg+10 / O+6
O+7 / O+6
10^{0}
10^{-1}
10^{-2}

Figure 9

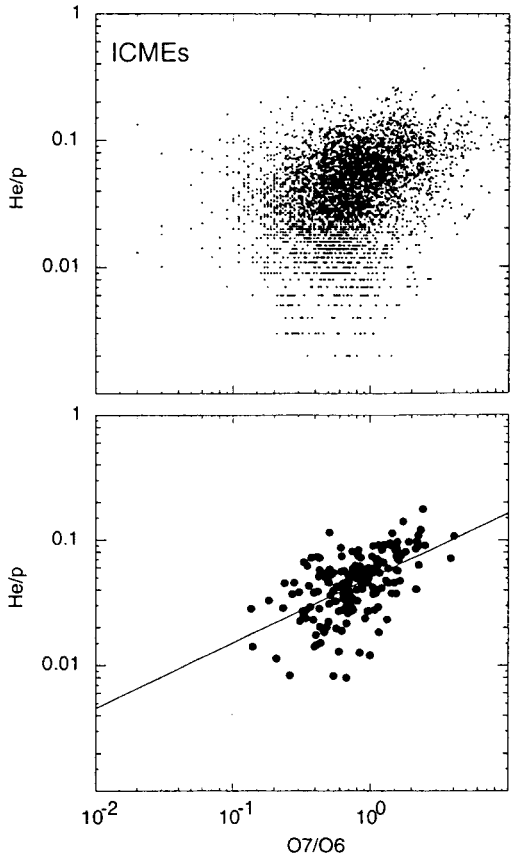

Figure 10